Spatial zoning of regional tsunami hazard and exposure in the Indian Ocean using scenario-based numerical tsunami simulation and global population data

Anawat Suppasri*, Tsuyoshi Futami**, Richard Sanders***, Fumihiko Imamura*

Abstract

The Indian Ocean is one of the tsunamigenic regions where the great earthquake occurred in 2004, with many smaller events reported each year thereafter. In addition, earthquakes in other subduction zones in Indonesia, Myanmar and Pakistan also have the potential to generate tsunamis that affect countries surrounding the Indian Ocean. Therefore, there is still a need to assess tsunami hazards level when zoning a given location's disaster planning and management. In this study, we summarize information regarding earthquake magnitude and recurrence. Then, the earthquake data is used as input for a numerical simulation to obtain tsunami hazard values, and global population data is used to assess the hazard for each country in the Indian Ocean. Most of the studied countries might be affected by a tsunami larger than 4 m generated by an M_w 9.0 earthquake, particularly India, Indonesia and Thailand, where the simulated resulting tsunami heights along the coast were larger than 16 m. The potential tsunami exposure (PTE) of the population distributions in the study area varied, with the highest PTE values in India, Indonesia and Myanmar, potentially exposing populations of over one million people. Large simulated tsunami heights in highly populated areas, such as Bangladesh, Indonesia and Pakistan, caused the highest hazard. This information is important for disaster planning and management against future tsunami in the Indian Ocean.

Keywords: Tsunami hazard assessment, tsunami simulation, population data, Indian Ocean tsunami

1. Introduction

Earthquake and tsunami activities are still found in the Indian Ocean after the great earthquake in 2004 initiated in the region and caused large impacts in the Andaman and North Sumatra. However, it is also important to study the tsunami hazards to populations from potential tsunamis in other regions that still have not been properly assessed. For example shown in Fig. 1, there are potential tsunami sources in Makran in Pakistan and Iran (Page et. al, 1979, Byrne et. al, 1992 and Heidarzadeh et al., 2008), Arakan in Myanmar (Socquet et al., 2006, Cummins, 2007, and Aung et al., 2008) and Java and Banda in Indonesia (Løvholt et al., 2006, Dominey-Howes et al., 2007, Jankaew et al., 2008, Monecke et al., 2008, Burbidge et al., 2008, Latief et al., 2008, Alam et al., 2012). This study was designed to assess the regional tsunami hazards among countries in the Indian Ocean using earthquake information, numerical tsunami simulations and global population data. Previous studies of earthquakes in the study area were referenced for information on the relationship between earthquake magnitude and return period. Numerical simulations were used to assist in estimating tsunami hazards based on earthquake parameters, and the exposure was assessed using

*International Research Institute of Disaster Science, Tohoku University, Japan
**Willis Japan Insurance Broker K.K.
***Willis (Singapore) Pte Ltd

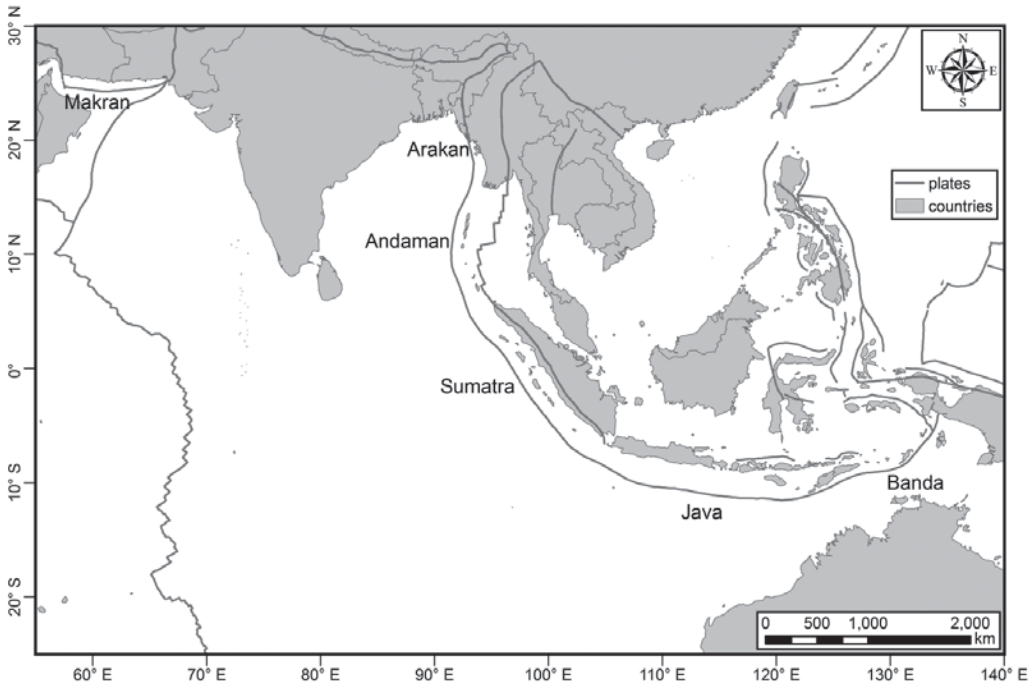

Fig. 1 Plate tectonics and subduction zones in the Indian Ocean

global population distribution data. The expected outputs are tables of tsunami hazard levels and maps giving information on tsunami height, earthquake magnitude or return period as well as hazard levels for the exposed population. These results will support for planning, management and policy development for regional tsunamis.

2. Data

2.1 Fault parameters

The authors considered far−field tsunamis, which are known to have occurred in the Indian Ocean. Subduction zones were considered as potential tsunami sources in that study, including the subduction zones in Makran, Arakan, Sumatra, Java and Banda. The present study assumed the strike, dip and slip values the same as a study by Okal et al. [2008] that considered seismological point of views based on mechanism of historical earthquakes in the study areas.

Papazachos et al. [2004] derived a series of empirical formulae to estimate the fault length (L), fault width (W) and displacement (u) that are based on the moment magnitude (M_w) of a given earthquake. The derived formulae were classified according to the type of fault. The following formulae were derived for calculating those fault parameters in the subduction zone:

Fault length, L (in km): $\log L = 0.55\ M_w - 2.19,\ 6.7 \le M_w \le 9.2$ (1)

Fault width, W (in km): $\log W = 0.31\ M_w - 0.63,\ 6.7 \le M_w \le 9.2$ (2)

Displacement, u (in cm): $\log u = 0.64\ M_w - 2.78,\ 6.7 \le M_w \le 9.2$ (3)

Table 1 Estimated size of each fault based on the earthquake moment magnitude

Magnitude (km)	Length (km)	Width (km)	Displacement (m)
M_w 9.3	1,000	200	14.86
M_w 9.0	600	175	9.55
M_w 8.9	500	160	8.24
M_w 8.7	400	150	6.14
M_w 8.5	300	135	4.57
M_w 8.2	200	120	2.94
M_w 7.6	100	100	1.21

For example, an M_w 7.6 earthquake will have a length of approximately 100 km, width of 50 km and displacement of 1.2 m. For convenience of the simulations, the present study simulated tsunamis that were generated by 7.6 and 9.3 M_w earthquakes using a unit of fault length of 100 km, as shown in Table 1. An earthquake with a 9.3 M_w was only applied to two regions, Andaman and Sumatra, following the 2004 Indian Ocean event.

2.2 Earthquake regions and return period

The study areas were separated into six regions based on geography: Makran, Arakan, Andaman, Sumatra, Java and Banda. General simulations of tsunami generated by 30 major historical earthquakes in the study area were previously performed by Suppasri et al. [2012a], showing the historical background of tsunami in this region. At the time of this study, the selected areas cover 24 zones of 17 African and Asian countries, as shown in Table 2. The number of scenarios for each earthquake magnitude and region is summarized in Table 3. For example, in the Andaman region (Fig. 2), the total length is 1,600 km (= 16 unit faults); therefore, 16 simulated scenarios exist for the M_w 7.6 case. For the 9.0 M_w simulations, the fault length of 600 km comprises 11 scenarios (nos. 1–6, nos. 2–7, nos. 3–8, nos. 4–9, nos. 5–10, nos. 6–11, nos. 7–12, nos. 8–13, nos. 9–14, nos. 10–15 and nos. 11–16). The total number of simulations performed in this study was 489 scenarios.

There have been some previous studies about earthquake return periods in the regions of the study area. In Makran, Page et al. [1979] first mentioned that the return period of a great event similar to the event that occurred in 1945 should be 125−250 years, while Byrne et al. [1992] estimated the same period as 175−300 years, and a recent study proposed a period of 250 years (Heidarzadeh et al. [2008]). However, a 9.0 M_w earthquake may or may not occur with a return period longer than 1,000 years [2008]. For Arakan, the great event that occurred in 1762 with an estimated M_w of 8.8 has a return period of 200 years (Cummins [2007]). The return periods for earthquakes of magnitudes 8.5 and 9.0 were estimated as 100 and 500 years, respectively (Socquet et al. [2006]). Aung et al. [2008] said that such an earthquake with an M_w of 8.8 in Arakan might have a return period of more than 1,000 years.

Researchers of the tsunami deposits after the great event in 2004 agreed that such an event might have a return period of 550−700 years (Jankaew et al. [2008]) or 600 years (Monecke et al. [2008]). The return period of an event of smaller magnitude (M_w 8.5) in the same region was estimated at 200 years (Løvholt et al. [2006]). Latief et al. [2008] considered four main subduction segments as tsunamigenic sources in Aceh, Seumelue, Andaman and Nias and proposed a hazard curve that correlates the earthquake return periods and the potential moment magnitudes. Their results agreed with

Table 2 Positions and zoning information for each studied country

Country	Zone	Lower−left (°E, °N)	Upper−right (°E, °N)
Australia	Australia	110.0, −25.0	143.0, −11.0
Bangladesh	Bangladesh	89.0, 20.7	92.3, 23.5
East Timor	East Timor	125.0, −9.5	127.5, −8.25
India	India (East)	79.5, 10.0	89.0, 20.7
	India (West)	68.2, 7.5	79.5, 24.0
	India (Nicobar)	91.5, 6.0	95.0, 15.0
Indonesia	Sumatra (North)	94.5, −3.5	100.0, 6.0
	Sumatra (South)	100.0, −6.2	106.0, 3.0
	Java	106.0, −11.5	125.0, −9.5
	Papua (West)	127.5, −9.0	141.0, 0.0
Iran	Iran	56.6, 25.0	61.62, 27.25
Malaysia	Malaysia	100.0, 3.05	102.0, 6.4
Maldives	Maldives	71.0, −1.0	75.0, 7.5
Mauritius	Mauritius	57.2, −20.6	57.9, −19.8
Myanmar	Myanmar (North)	92.3, 15.0	95.0, 20.7
	Myanmar (South)	95.0, 10.0	99.0, 18.0
Oman	Oman	55.0, 17.0	60.0, 25.0
	Oman (North)	56.0, 25.6	56.6, 26.5
Pakistan	Pakistan	61.62, 23.7	68.17, 25.5
Seychelles	Seychelles	55.0, −5.0	56.0, −4.0
Reunion	Reunion	55.1, −21.5	56.0, −20.7
Sri Lanka	Sri Lanka	79.5, 5.5	82.5, 10.0
Thailand	Thailand	94.5, 6.4	100.0, 10.0
UAE	UAE	56.25, 25.0	56.4, 25.6

Table 3 Number of simulation scenarios for each earthquake magnitude in each region

Region	Number of simulation scenario for each earthquake magnitude							**Total**
	M_w 9.3	M_w 9.0	M_w 8.9	M_w 8.7	M_w 8.5	M_w 8.2	M_w 7.6	
Makran		4	5	6	7	8	9	**39**
Arakan		2	3	4	5	6	7	**27**
Andaman	7	11	12	13	14	15	16	**88**
Sumatra	20	24	25	26	27	28	29	**179**
Java		10	11	12	13	14	15	**75**
Banda		11	12	13	14	15	16	**81**
Total	**27**	**62**	**68**	**74**	**80**	**86**	**95**	**489**

those of Jankaew et al. [2008], Monecke et al. [2008] and Løvholt et al. [2006] were used in this study. Burbidge et al. [2008] derived hazard curves representing earthquake return periods as a function of magnitude in Java, Sumatra, Nankai, Seram and South Chile. The present study used their results for the earthquake return periods in Java and nearby regions. The information about earthquake magnitudes and return periods derived from previous studies is summarized in Table 4.

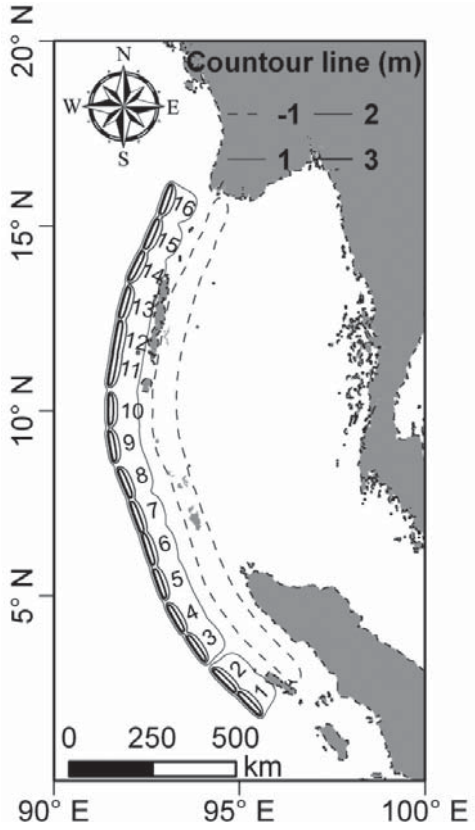

Fig. 2 The location of 16 faults divided into 100−km lengths in the Andaman region

Table 4 Summary of earthquake magnitude and return periods for each region

Mw	Earthquake return period (year)					
	Makran [A]	Arakan [B,C,D]	Andaman [E,F,G]	Sumatra [E,F,G]	Java [H]	Banda [H]
9.3	**N/A**	**N/A**	600	600	**N/A**	**N/A**
9.0	**N/A**	500	450	450	1,000	1,200
8.9	**N/A**	350	400	400	800	1000
8.7	**N/A**	200	325	325	500	600
8.5	1,000	100	250	250	300	400
8.2	400	40	170	170	150	200
7.6	65	5	65	65	40	50

[A] Heidarzadeh et al., 2008
[B] Aung et al., 2008
[C] Socquet et al., 2006
[D] Cummins, 2007
[E] Jankaew et al., 2008
[F] Monecke et al., 2008
[G] Latief et al., 2008
[H] Burbidge et al., 2008

2.3 Global bathymetry and population data

This study used global bathymetry data for a 1 arc−minute grid (approximately 2 km) provided by the General Bathymetric Chart of the Oceans (GEBCO, [2009]) and global population data called LandScan for a 30 arc−second grid (approximately 1 km) provided by the Oak Ridge National Laboratory [2009]. The GEBCO data are largely based on the most recent set of bathymetric contours contained within the GEBCO Digital Atlas and are now widely used in many numerical tsunami simulations including

areas in the Indian Ocean such as in southeast Asia (Thio et al., 2007), Thailand (Løvholt et al., 2006 and Suppasri et al., 2011) Indonesia (Koshimura et al., 2009 and Muhari et al., 2011), Sri Lanka (Goto et al., 2011) and Iran and Pakistan (Heidarzadeh et al., 2008, Yanagisawa et al., 2009 and Heidarzadeh and Kijko, 2010). The LandScan data are the finest-resolution global population distribution data available and represent an ambient population which averaged over 24 hours (Oak Ridge National Laboratory [2009]).

3. Method

3.1 Tsunami numerical simulation method

A method proposed by Mansinha and Smylie [1971] was used to calculate the seafloor deformations from the earthquake fault parameters, as mentioned in the previous section. In general, seafloor deformation is the initial tsunami profile for a tsunami simulation because it is assumed that the water column over the seafloor cannot escape within a short duration of earthquake generation (IUGG/IOC TIME Project, [1997]). A series of tsunami scenarios were simulated using the TUNAMI model developed at Tohoku University (IUGG/IOC TIME Project, [1997]), which is widely used in many countries. The model contains sets of linear shallow-water wave equations that are solved using a finite difference scheme in spherical coordinates that neglects effects from bottom friction and fault rupture velocity. The inputs for the model were the fault parameters and the global bathymetry data from GEBCO, as mentioned in the previous section. Results from the simulation at this stage is maximum tsunami heights along shoreline of the study areas.

3.2 Tsunami exposure searching method

The maximum tsunami height along the coastlines simulated using the numerical simulation was on a 2 km grid, and the LandScan global population data were available on a 1 km grid. Two problems had to be solved: (1) searching and estimating the tsunami runup height along the coast and (2) creating a different grid resolution. This study followed the method proposed by Suppasri et al. [2012b] and Suppasri et al. [2012c] to identify population exposure and count the population numbers along coastlines. The method relied on a numerical filter to search a coastline grid. The inland runup height next to a coastal grid was estimated by averaging the surrounding tsunami heights along the shoreline and then project the average height inland as the runup height (Fig. 3). The Global population grid was overlaid on the estimated runup height grid. The possible exposure of a population was

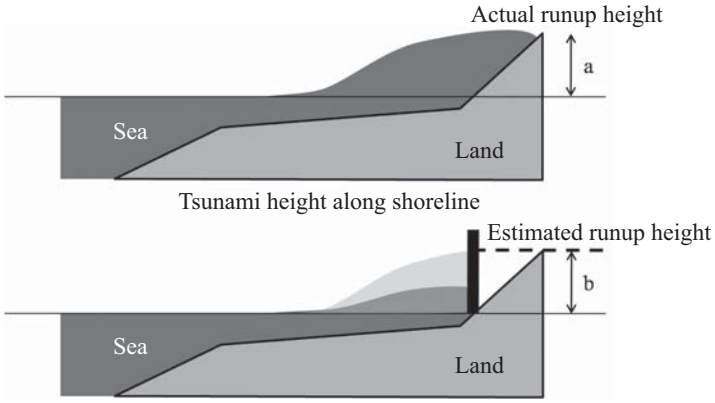

Fig. 3 Calculation description of tsunami height alone shoreline and runup height for (a) actual condition and (b) far-field tsunami simulation and projected runup height

Table 5 Proposed hazard level based on the tsunami height and population density

Category	Population per km^2	= 1	< 5	< 10	< 50	< 100	< 500	< 1,000	< 5,000	< 10,000	> 10,000
Height (m)	Level	1	2	3	4	5	6	7	8	9	10
< 0.125	1	1	2	3	4	5	6	7	8	9	10
< 0.25	2	2	4	6	8	10	12	14	16	18	20
< 0.5	3	3	6	9	12	15	18	21	24	27	30
< 1	4	4	8	12	16	20	24	28	32	36	40
< 2	5	5	10	15	20	25	30	35	40	45	50
< 4	6	6	12	18	24	30	36	42	48	54	60
<8	7	7	14	21	28	35	42	49	56	63	70
< 16	8	8	16	24	32	40	48	56	64	72	80
< 32	9	9	18	27	36	45	54	63	72	81	90
> 32	10	10	20	30	40	50	60	70	80	90	100

counted and estimated along the tsunami−prone coastlines where the estimated runup height is higher than the land elevation using 1 km grid distances due to the resolution of the global population data.

3.3 Population exposure assessment method

Because a population's exposure depends on the tsunami hazard and population exposure, this study proposed a new hazard assessment criteria based on tsunami hazard and exposed population as shown in Table 5. For the calculation of the hazard level, we used a hazard level from one to ten for both the tsunami runup height and exposed population per square kilometer, respectively. The categories for the tsunami runup height were less than 0.125 m to greater than 32 m. The values for the number of people per square kilometer were from 1 to greater than 10,000.

The total hazard level is a product of the levels from the tsunami runup height and exposed population per square kilometer. Therefore, the maximum hazard level is 10 × 10 = 100 using these criteria, which is easy to understand and compare. In addition, the hazard levels of 1−10, 11−30 and 31−100 are assumed to represent a low, medium and high hazard, respectively, because each level contains approximately one−third of the total distribution of levels. For example, a 0.5 m tsunami runup with an affected population of 10 (hazard level = 3 × 3 = 9) will be considered as low hazard, a 2 m tsunami with an affected population of 100 (hazard level = 5 × 5 = 25) will be medium hazard, and a 8 m tsunami with an affected population of 1,000 (hazard level = 7 × 7 = 49) will be high hazard.

4. Results

4.1 Tsunami hazard curves

Tsunami hazard curves can be obtained by plotting the simulated maximum tsunami height against the earthquake magnitude or return period. Fig. 4a shows an example from Sri Lanka, which is affected by tsunamis from several directions, e.g., from Makran in the west and from Arakan−Andaman−Sumatra−Java in the east. The maximum simulated tsunami height caused by an M_w 9.0 earthquake was approximately 10 m in Andaman. Tsunami generated by earthquakes in Arakan and Sumatra do not propagate in a straight direction to Sri Lanka, leading to a maximum tsunami height of approximately 3−5 m. The maximum tsunami height driven by earthquakes from Makran was only approximately 1 m in Java that are far away and are not in the direct route of wave propagation. The simulated tsunami height became smaller as the earthquake magnitude decreased and was less than 1 m for an M_w 7.6 earthquake for all of the studied regions.

Figs. 4b−4d show other examples in Mauritius, North Sumatra and Northwest Australia. Mauritius is located in the Southwest Indian Ocean, where no effect of tsunamis from Arakan and Banda would occur due to its geographic position. Sumatra can also be affected by tsunamis from throughout the region except for the Makran region because of its geographical location. Tsunamis affecting Australia could stem from Andaman in the northwest to Banda in the north. Mauritius and Australia have similar trends with maximum tsunami heights for M_w 8 and 9 class earthquakes of 1 m and 10 m, respectively. However, the same class of earthquake might cause tsunami heights from 3 to 30 m for Sumatra, Indonesia.

Figs. 5a−5d show the tsunami hazard curves for the aforementioned regions when plotting the earthquake return period. For example, the maximum tsunami height in the next 100 and 500 years might be approximately 1 m and 7−10 m, respectively, for Sri Lanka, Mauritius and Northwest Australia but would be 3 m and more than 20 m in North Sumatra, Indonesia.

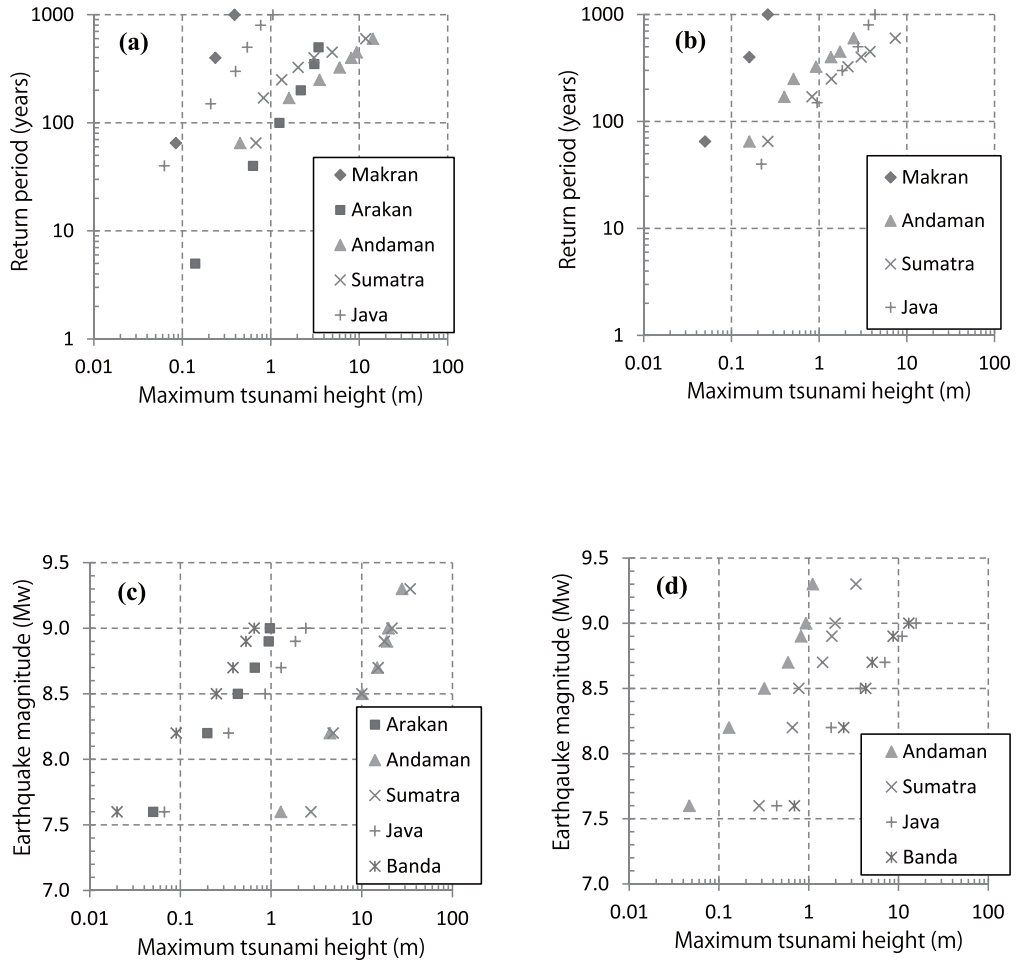

Fig. 4 Examples of tsunami hazard curves as a function of earthquake magnitude (M_w) in (a) Sri Lanka, (b) Mauritius, (c) North Sumatra, Indonesia and (d) Northwest Australia

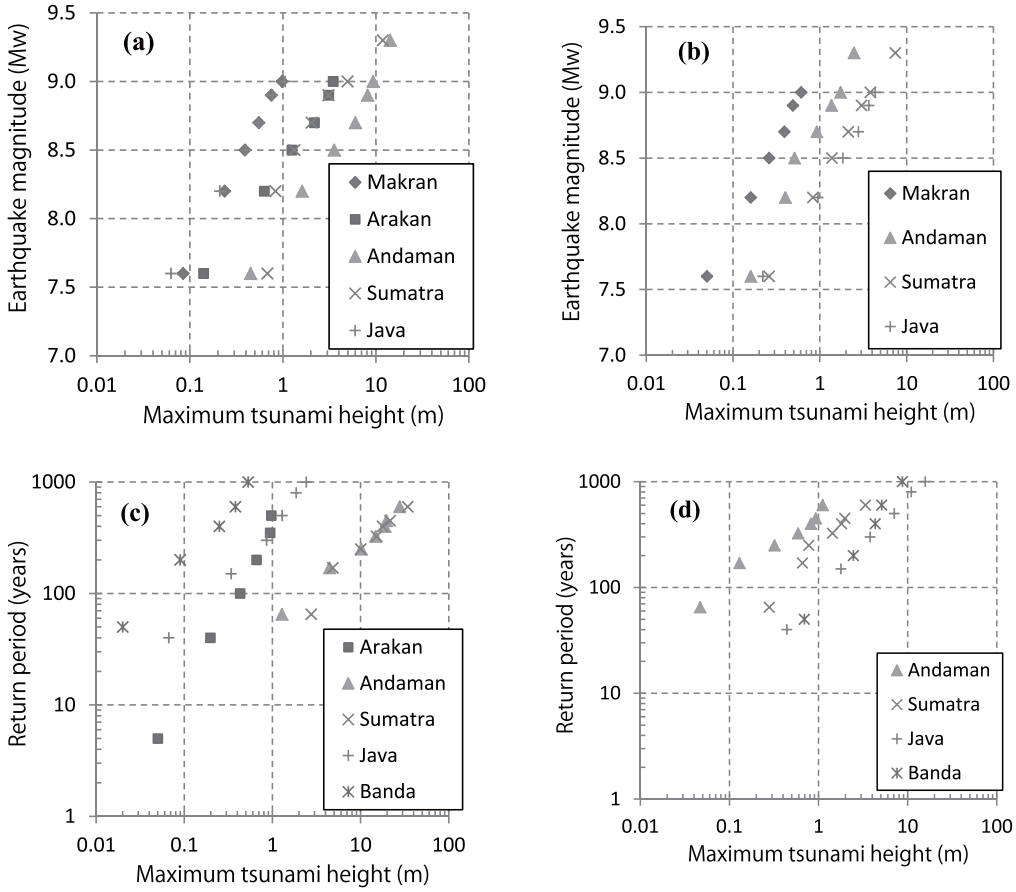

Fig. 5 Examples of tsunami hazard curves as a function of earthquake return period in (a) Sri Lanka, (b) Mauritius, (c) North Sumatra, Indonesia and (d) Northwest Australia

Comparison of the simulation results from this study and other studies is discussed here. The maximum tsunami height of 11−14 m was obtained by this study in Makran region including Iran and Pakistan, where 7−10 m, 12−15m and more than 10 m were reported by Page et al. [1979], Heidarzadeh et al. [2008] and Yanagisawa et al. [2009] respectively. Cummins [2007] estimated the maximum offshore tsunami height up to 10 m based on M_w 8.8 earthquake while this study got around 7−8 m in the same coastal area in Myanmar from M_w 8.7 and 8.9 earthquakes. In Thailand, the simulated maximum tsunami height by this study was about 0.3 and 3 m by M_w 7.6 and 8.5 earthquakes in Andaman where Løvholt et al. [2006] estimated as 0.2−0.5 and 1−2 m by M_w 7.5 and 8.5 earthquakes in the same source region respectively. These are similar to a study by Suppasri et al. [2012c] that estimated the maximum tsunami height as 0.3−0.4 and 2−3 m for M_w 7.6 and 8.5 earthquakes accordingly.

There are some regions in Indonesia to be compared namely Sumatra, Java and Sulawesi. For Aceh province in the North Sumatra region, this study estimated about 3, 10 and more than 10 m for the case of M_w 7.6, 8.5 and > 9.0 earthquakes while Thio et al. [2007] and Latief et al. [2008] estimated as 1−2, 7−8 and 10 m or more respectively. A study by Hartanto [2013] reported the possible maximum height in Padang in the central Sumatra as about 1 m and 7−14 m for M_w 8.1 and 8.9 earthquakes respectively. For

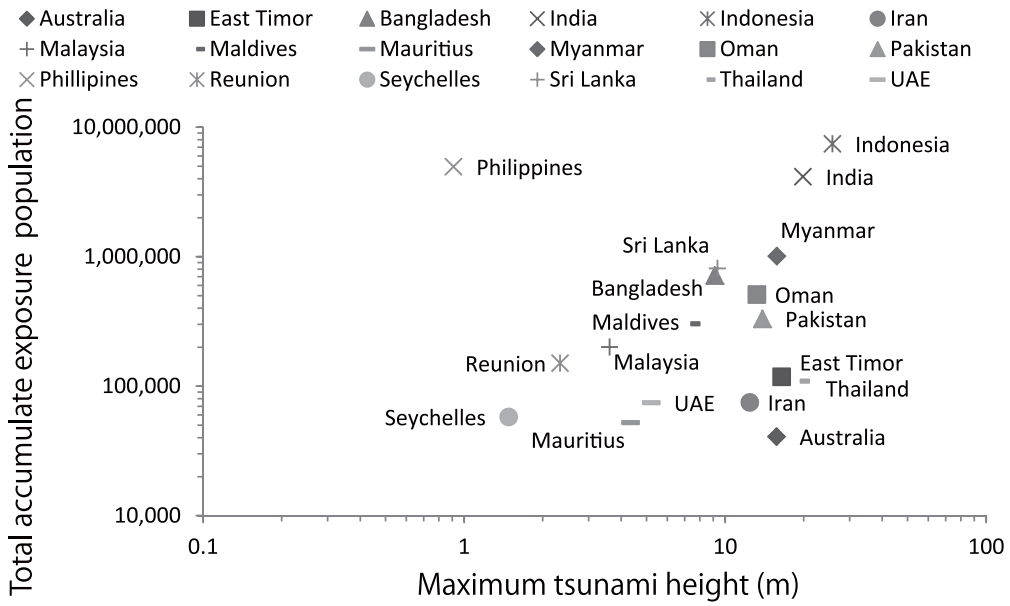

Fig. 6 Simulated maximum tsunami height and total accumulated exposure of the local population for a M_w 9.0 earthquake by country

Java region, our results also agreed with other studies as the estimated the maximum tsunami height is about 1−2 m by M_w 7.7 earthquake when compared with Cipta [2008] and more than 10 m by M_w 8.8 earthquake when compared with Prasetya [2009]. In Sulawesi, earthquake in Java generated the maximum tsunami height of less than 2 m in any case which agreed with the results from Thio et al. [2007]. In the northwestern Australia, the simulation results from this study is about 1−2 m height from earthquake in Andaman and Sumatra however, it can be up to 10 m or more in some cases from the earthquake sources in Java and Banda. On the other hand, Berbidge et al. [2008] showed in their results that the maximum simulated offshore wave height was about 2 m or more which the runup can be many times greater than this value.

4.2 Maximum tsunami height, exposure population and hazard map

Further analysis of the results of the maximum tsunami height and exposure levels of the studied populations is discussed here. Fig. 6 shows an example of a plot of the simulated maximum tsunami height and total accumulated exposure of the population within a 1 km inundation distance by country for an M_w 9.0 earthquake. For more than half of the countries in the study area, it is possible to have a maximum tsunami height equal or greater than 10 m with an exposed population of over 100,000 (Fig. 6), with the exception of countries that are far from the tsunami sources, such as small islands in the southwest Indian Ocean.

We can classify these countries into four groups based on their population exposure using a tsunami generated by an M_w 9.0 earthquake as an example. The two countries with the highest hazard, considering separately the highest class of tsunami height and exposed population, are Indonesia and India, which form the first group. The simulated tsunami height was more than 20 m, and the exposed population reached 4−7 million for these two countries. The second group was primarily populated countries, such

as Bangladesh, Maldives, Myanmar, Oman, Pakistan and Sri Lanka, where the simulated tsunami height was approximately 10 m with an exposed population of slightly less than a million. The third group is similar to the second group with a similar simulated tsunami height but a comparatively lower expose population level of approximately 0.1 million: Australia, East Timor, Iran and Thailand. The last group is composed of countries, including Malaysia, Mauritius, Reunion, Seychelles and UAE, that are far from tsunami sources and might experience tsunami less than 5 m with exposed populations of approximately 0.1 million.

A tsunami hazard map showing the maximum tsunami height simulated for each scenario with the same earthquake magnitude was overlaid on the other maps to determine the maximum tsunami height based on the given scenarios in each grid. For example, there were 62 scenarios for an M_w 9.0 earthquake, and Fig. 7 shows the hazard map as a result of overlaying 62 maps. The map shows a possible worst case of the maximum of the maximum simulated tsunami heights for an M_w 9.0 earthquake. Large tsunami heights were found along the coastlines of the Indian Ocean, except the west coast of India. Fig. 7 also shows the distribution of the population data in the study area. Large populations are found throughout India and on Java in Indonesia.

Comparisons of the simulated maximum tsunami heights (by M_w 9.0 or 9.3 earthquakes) and recorded tsunami heights (NOAA database, [2012]) from the 1945 Makran and 2004 Indian Ocean tsunami are shown in Table 6. The simulated results show similar or higher maximum tsunami heights than the recorded data in most of the studied countries. At the very least, we showed that the simulated maximum tsunami heights for each country are reliable and compatible with historical records. The results also might be applicable for those countries that still have no recent tsunami experience or historical tsunami record to guide their preparation.

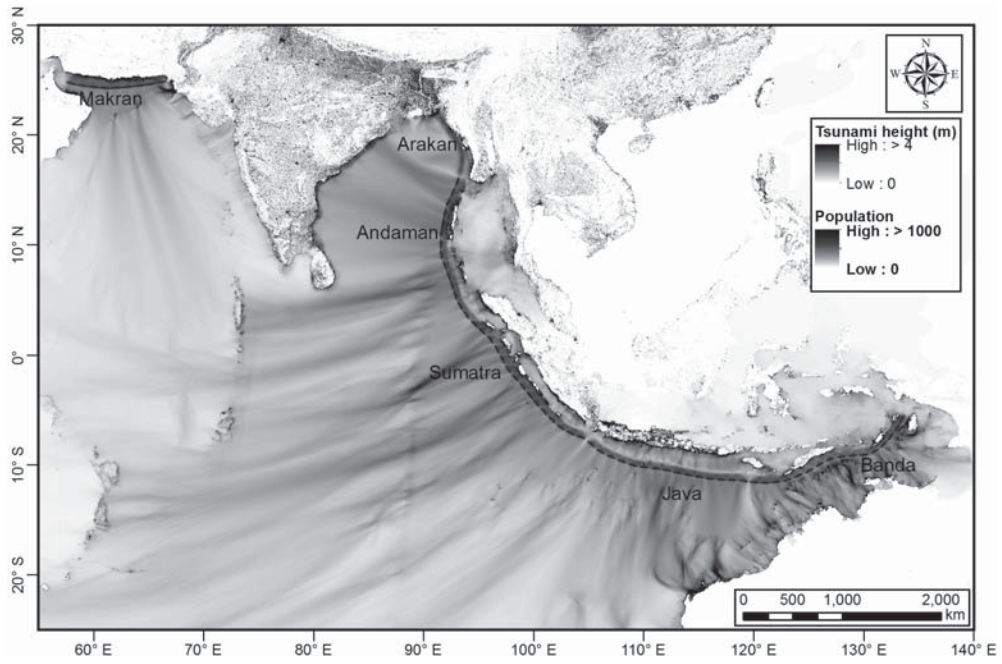

Fig. 7 Total 62 maximum tsunami height maps for a M_w 9.0 earthquake overlaid with the population distri−bution in the study area

4.3 Regional population hazard levels

A hazard level for each coastal grid was calculated based on the criteria given in section 3.3. This value is a representative of the maximum value among values in other grids for each country. Fig. 8 shows an example of the maximum hazard level for each zone for 7.6−9.3 M_w earthquakes in Andaman. If we compare the results from the M_w 9−class (M_w 8.7−9.3) earthquakes, the hazard levels of Bangladesh, India, Indonesia (Sumatra), Maldives, Myanmar, Sri Lanka and Thailand were similar because their average values ranged from 50 to 70. The hazard level of 50−70 means, for example, that a tsunami height of 2−8 m may occur in an area with a population of more than 10,000 people/km^2 or a tsunami larger than 32 m may occur in an area with a population ranging from 100−1,000 people/km2. Other regions, such as Australia, Indonesia (Java), Iran, Pakistan, Oman and islands in the Southwest Indian Ocean, suffer fewer effects from tsunami in Andaman due to their locations.

The maximum hazard level calculated for each region from each tsunami source is useful when comparing the tsunami hazard to population among countries. An example for Sri Lanka is shown in Fig. 9, which demonstrates the maximum tsunami height from M_w 9.0 earthquakes, the population distribution and the maximum hazard level for each coastal grid. These results also help to make a comparison based on the population hazard information within a country.

4.4 Assumptions and limitations

In terms of the fault parameters, this study only limited the fault position related parameters such as strike, dip, slip and depth for only one pattern based on the mechanism of historical earthquakes proposed by previous studies for each unit fault along the Indian Ocean. Also the fault geometry was limited to every 100 km length of the fault for a convenience in setting the

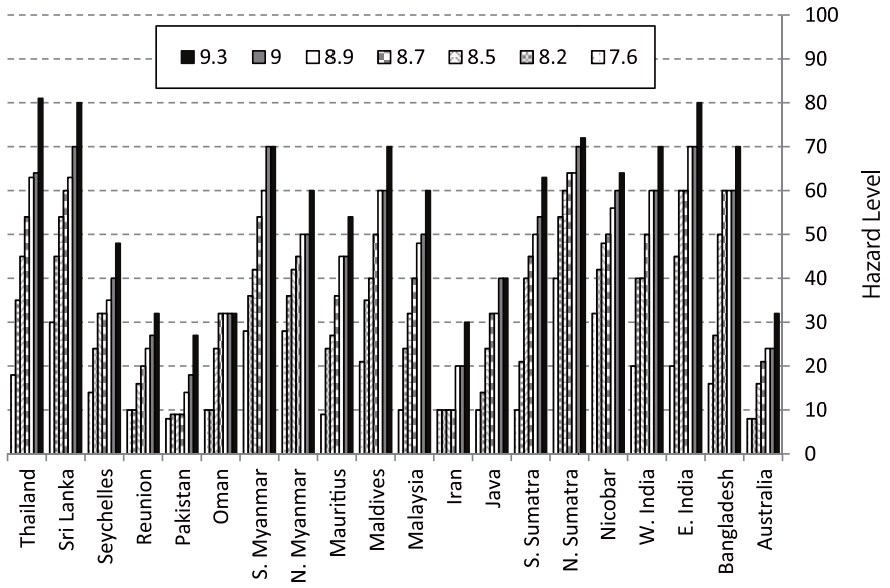

Fig. 8 Maximum population hazard level for each zone by tsunamis generated from 7.6−9.3 M_w earthquakes in Andaman

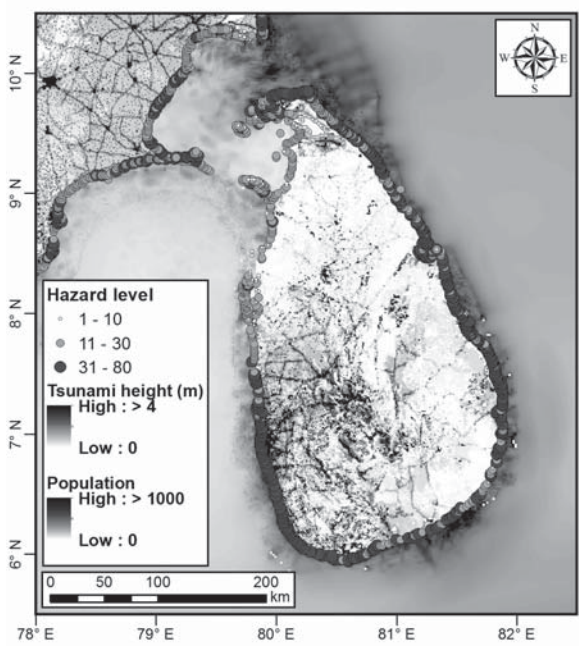

Fig. 9 Distribution of the calculated population hazard levels by tsunamis generated from 9.0 M_w earth−quakes in Sri Lanka

calculation. Therefore, earthquakes in the future may occur with fault parameters differ from what assumed in this study or may not follow the empirical relationship between the earthquake moment magnitude and the fault geometry and the dislocation. For the far−field simulation point of view, because of the scope that is to focus on the regional or macro scale, we used the linear shallow−water wave equations to estimate the maximum tsunami height along the shoreline and inland runup height in a coarse computational grid which might may not as accurate as the results of the simulation that includes the non−linear effect for the tsunami inundation over the land in a very find grid. In addition, although we only count the number of exposed population in a grid that the runup height is higher than the land elevation, the effect of day or night time population could not be represented in the present data.

5. Conclusions

Based on the maximum tsunami population hazard level for each of the regions and countries stemming from M_w 9.0 earthquakes in all of the possible tsunamigenic regions, we summarized the regions as shown in Figs. 10−12 and Table 6. Figs. 10−12 summarize an example overview of the tsunami hazard (Fig. 10), population exposure (Fig. 11) and hazard level (Fig. 12) of probable tsunamis from 62 scenarios of M_w 9.0 earthquakes in the Indian Ocean. Most of the studied countries might be affected by a tsunami larger than 4 m generated by an M_w 9.0 earthquake (Fig. 10). In India, Indonesia and Thailand, the simulated tsunami heights are larger than 16 m. The potential tsunami exposures (PTE) of the population distributions in the study area vary, with the highest PTE in India, Indonesia and Myanmar, with PTE populations larger than one million (Fig. 11). Finally, a comparison of the population hazard levels considering both runup height and exposed population is shown in Fig. 12. Large simulated tsunami heights in highly populated areas, such as Bangladesh, Indonesia and Pakistan, are shown to cause

the highest hazards. Details of the calculated tsunami population hazard levels from an M_w 9.0 earthquake for each of the studied regions are summarized in Table 6. The findings from this study can be a decision support tool to help with zoning and to compare the regional tsunami hazards among the countries surrounding the Indian Ocean.

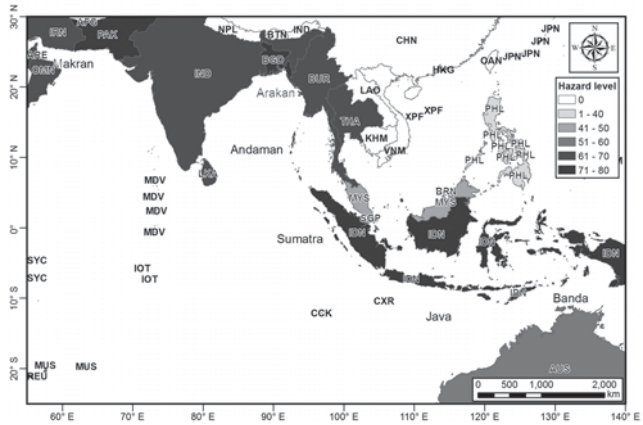

Fig. 10 Zoning of countries based on the simulated maximum tsunami height

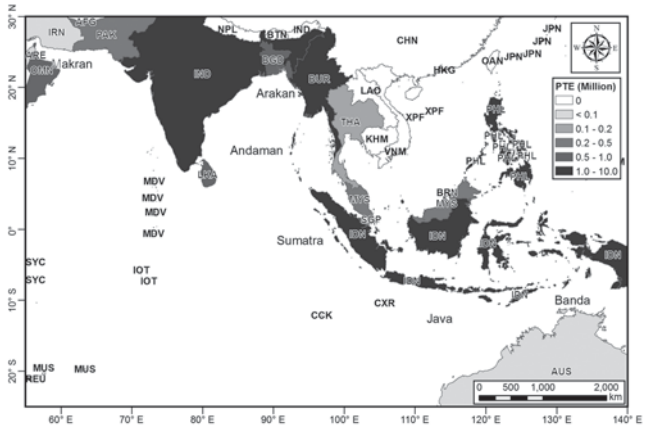

Fig. 11 Zoning of countries based on the total number of potential tsunami exposures

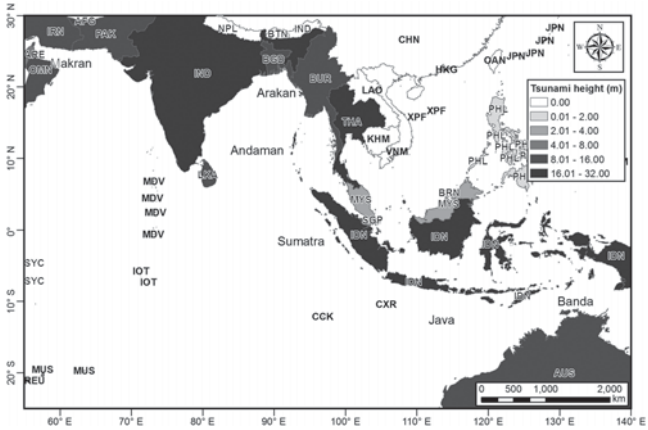

Fig. 12 Zoning of countries based on the calculated population hazard level

Table 6 Summary of all of the results in all of the studied zones and countries: the maximum tsunami height (historical database and simulations) for an M_w 9.0 earthquake and the maximum risk level of the areas

Location		Max. tsunami height (m)		Maximum tsunami population hazard level							
Country	Zone	Max. from database (region)	Max. simulated by this study (source region)	Makran > 1000 yrs	Arakan 500 yrs	Andaman 450 Yrs	Sumatra 450 yrs	Java 1000 yrs	Banda > 1000 yrs	MAX Region	Country MAX
Australia	Australia	0.90	15.74 (Java)			24	40	56	56	56	56
Bangladesh	Bangladesh		9.13 (Arakan)		80	60	40	35		80	80
East Timor	East Timor		16.46 (Banda)					36	70	70	70
India	E. India	9.56	20.16 (Andaman)		70	70	60	35		70	70
	W. India		6.66 (Andaman)	60		60	60	40		60	
	Nicobar		34.78 (Andaman)		36	60	48	20		60	
Indonesia	N. Sumatra	50.9	34.28 (Sumatra)		32	70	72	40	24	72	80
	S. Sumatra		37.09 (Sumatra)			54	80	60	40	80	
	Java		31.06 (Banda)				56	80	72	80	
	W. Papua		24.21 (Banda)					40	70	70	
	Borneo		1.12 (Banda)					24	32	32	
	Sulawesi		11.97 (Banda)					40	64	64	
Iran	Iran		12.42 (Makran)	70		20				70	70
Malaysia	Malaysia	4.00	5.46 (Sumatra)		30	50	40			50	50
Maldives	Maldives	4.43	8.82 (Andaman)	40	18	60	50	32		60	60
Mauritius	Mauritius		7.40 (Sumatra)	18		45	54	54		54	54
Myanmar	N. Myanmar	2.90	15.77 (Arakan)		70	50	32			70	70
	S. Myanmar		19.65 (Andaman)		40	70	40			70	
Oman	Oman	1.65	13.23 (Makran)	70		32	24			70	70
	N. Oman		3.46 (Makran)	48						48	
Pakistan	Pakistan	15.24	13.90 (Makran)	72		18				72	72
Philippines	Philippines		0.91 (Banda)						40	40	40
Reunion	Reunion		3.74 (Sumatra)			27	50	40		50	50
Seychelles	Seychelles	1.39	2.33 (Sumatra)	40		40	40			40	40
Sri Lanka	Sri Lanka	11.3	14.25 (Andaman)	40	48	70	60	40		70	70
Thailand	Thailand	19.57	36.78 (Andaman)		48	64	54			64	64
UAE	UAE		5.21 (Makran)	63						63	63

Acknowledgments

This study was sponsored by the Willis Research Network as part of the Pan Asian/Oceanian Tsunami Risk Modeling and Mapping Project. The authors appreciate the kind cooperation of Ms. Tae Asada throughout the study. The authors also express profound gratitude for very useful comments and suggestions from Dr. Dale Dominey-Howes from the University of New South Wales.

References

Alam, E., Dominey-Howes, D., Chagué-Goff, C. and Goff, J. [2012] "Tsunamis of the northeast Indian Ocean with a particular focus on the Bay of Bengal – a synthesis and review," Earth Science Reviews, 114, 175-193.

Aung, T. T., Satake, K., Okamura, Y. and Shishikura, M. [2008] Geologic evidence for three great earthquakes in the past 3400 years Off Myanmar," Journal of Earthquake and Tsunami, 2, 259–265.

Burbidge, D., Cummins, P. R., Mleczko, R. and Thio, H. K. [2008] "Probabilistic tsunami hazard assessment for Western Australia," Pure and Applied Geophysics, 165, 2059–2088.

Byrne, D. E., Sykes, L. R. and Davis, D. M. [1992] "Great thrust earthquakes and aseismic slip along the plate boundary of the Makran subduction zone," Journal of Geophysical Research, 97, 449–478.

Cipta, A. [2008] "Study on tsunami numerical modeling for making tsunami hazard maps in Indonesia," Bulletin of IISEE, 43, 127-132.

Cummins, P.R. [2007] "The potential for giant tsunamigenic earthquakes in the northern Bay of Bengal," Nature, 449, 75–78.

Dominey-Howes, D., Cummins, P. and Burbidge, D. [2007] "Historic records of teletsunami in the Indian Ocean and insights from numerical modeling," Natural Hazards, 42, 1-17.

General Bathymetric Chart of the Oceans (GEBCO), GEBCO_08 grid: http://www.gebco.net/ (20 February 2009)

Goto, K., Takahashi, J., Oie, T. and Imamura, F. [2011] "Remarkable bathymetric change in the nearshore zone by the 2004 Indian Ocean tsunami: Kirinda Harbor, Sri Lanka," Geomorphology, 127 (1-2) 107-116.

Hartanto, D. [2013] "Tsunami simulations off the west coast of Sumatra using dispersive and non-dispersive waves," Bulletin of IISEE, 47, 109-114.

Heidarzadeh, M., Pirooa, M. D., Zaker, N. H., Yalciner, A. C., Mokhtari, M. and Esmaeily, A. [2008] "Historical tsunami in the Makran subduction zone off the southern coasts of Iran and Pakistan and results of numerical modeling," Ocean Engineering, 35, 774–786.

Heidarzadeh, M. and Kijko, A. [2010] "A probabilistic tsunami hazard assessment for the Makran subduction zone at the northwestern Indian Ocean," Natural Hazards, 56(3), 577-593.

IUGG/IOC TIME Project, Numerical Method of Tsunami Simulation with the Leap-Frog Scheme, UNESCO Intergovernmental Oceanographic Commission Manuals and Guides, 35 (1997), 126p.

Jankaew, K., Atwater, B.F., Sawai, Y., Choowong, M., Charoentitirat, T., Martin, M.E. and Prendergast, A. "Medieval forewarning of the 2004 Indian Ocean tsunami in Thailand," Nature, 455 (2008), 1228–1231.

Koshimura, S., Oie, T., Yanagisawa, H., and Imamura, F. [2009] "Developing fragility curves for tsunami damage estimation using numerical model and post-tsunami data from Banda Aceh, Indonesia," Coastal Engineering Journal, 51, 243–273.

Latief, H., Sengara, I.W., Kusuma, S.B. [2008] "Probabilistic seismic and tsunami hazard analysis model for input to tsunami warning and disaster mitigation strategies," In

proceedings of the International Conference on Tsunami Warning (ICTW) Bali, Indonesia.

Løvholt, F., Bungum, H., Harbitz, C. B., Glimsdal, S., Lindholm, C.D. and Pedersen, G. [2006] "Earthquake related tsunami hazard along the western coast of Thailand," Natural Hazards and Earth System Sciences, 6, 979–997.

Mansinha, L. and Smylie, D.E. [1971] "The displacement fields of inclined faults. Bulletin of the Seismological Society of America," 61, 1433–1440.

Monecke, K., Finger, W., Klarer, D., Kongko, W., McAdoo, B.G., Moore, A.L., Sudrajat, S.U. [2008] "A 1,000–year sediment record of tsunami recurrence in northern Sumatra," Nature, 455, 1232–1234.

Muhari, A., Imamura, F., Koshimura, S. and Post, J. [2011] "Examination of three practical run−up models for assessing tsunami impact on highly populated areas, Natural Hazards and Earth System Sciences, 11, 3107−3123.

National Geophysical Data Center (NGDC), Tsunami database: http://www.ngdc.noaa.gov/hazard/tsu_db.shtml (6 August 2012)

Oak Ridge National Laboratory, LandScan2008, http://www.ornl.gov/sci/landscan/ (13 October 2009)

Okal, E.A. and Synolakis, C.E. [2008] "Far−field tsunami hazard from mega−thrust earthquakes in the Indian Ocean," Geophysical Journal International, 172 (2008) 995−1015.

Page, W.D., Alt, J. N., Cluff, L. S. and Plafker, G. [1979] "Evidence for the recurrence of large−magnitude earthquakes along the Makran coast of Iran and Pakistan," Tectonophysics, 52, 533–547.

Papazachos, B. C., Scordilis, E. M., Panagiotopoulos, D. G., Papazachos, C. B. and Karakaisis, G. F. [2004] "Global relations between seismic fault parameters and moment magnitude of earthquakes," Bulletin of the Geological Society of Greece ,vol. 36, Proc. of the 10th International Congress, Thessaloniki, Greek.

Prasetya, T. [2009] "Numerical simulation for the assessment of tsunami scenarios in southern Yogyakarta, central Java Island, Indonesia," Bulletin of IISEE, 44, 121−126.

Socquet, A., Vigny, C., Chamot−Rooke, N. and Simons W. [2006] "India and Sunda plates motion and deformation along their boundary in Myanmar determined by GPS," Journal of Geophysical Research, 111, B05406.

Suppasri, A., Koshimura, S. and Imamura, F. [2011] "Developing tsunami fragility curves based on the satellite remote sensing and the numerical modeling of the 2004 Indian Ocean tsunami in Thailand," Natural Hazards and Earth System Sciences, 11, 173–189.

Suppasri, A., Futami, T., Tabuchi, S. and mamura, F. [2012a] "Mapping of historical tsunamis in the Indian and Southwest Pacific Oceans," International Journal of Disaster Risk Reduction, 1, 62−71.

Suppasri, A., Imamura, F. and Koshimura, S. [2012b] "Tsunami hazard and casualty estimation in a coastal area that neighbors the Indian Ocean and South China Sea," Journal of Earthquake and Tsunami, 6, 1250010.

Suppasri, A., Imamura, F. and Koshimura, S. [2012c] "Probabilistic tsunami hazard analysis and risk to coastal populations in Thailand," Journal of Earthquake and Tsunami, 6, 1250011.

Thio, H. K., Somerville, P. and Ichinose, G. "Probabilistic analysis of strong ground motion and tsunami hazards in southeast Asia," Journal of Earthquake and Tsunami, 1 (2), 119−137.

Yanagisawa, H., Koshimura, S., Imamura, F., Watabe, H., and Egashira, T. [2009] "Tsunami hazard assessment along the coast of Pakistan based on the 1945 Makran tsunami," Journal of Japan Society of Civil Engineers, Ser. B2 (Coastal Engineering), 65, 1, 306−310.